

## Bottleneck Effects in Turbulence: Scaling Phenomena in $r$ versus $p$ Space

Detlef Lohse<sup>1,\*</sup> and Axel Müller-Groeling<sup>2,†</sup>

<sup>1</sup>The James Franck Institute, The University of Chicago, 5640 South Ellis Avenue, Chicago, Illinois 60637

<sup>2</sup>Department of Physics, University of Toronto, 60 St. George Street, Toronto, Ontario M5S 1A7, Canada

(Received 4 May 1994)

We (analytically) calculate the energy spectrum corresponding to various experimental and numerical turbulence data analyzed by Benzi *et al.* We find two bottleneck phenomena: While the local scaling exponent  $\zeta_r(r)$  of the structure function decreases monotonically, the local scaling exponent  $\zeta_p(p)$  of the corresponding spectrum has a minimum of  $\zeta_p(p_{\min}) \approx 0.45$  at  $p_{\min} \approx (10\eta)^{-1}$  and a maximum of  $\zeta_p(p_{\max}) \approx 0.77$  at  $p_{\max} \approx 8L^{-1}$ . A physical argument starting from the constant energy flux in  $p$  space reveals the general mechanism underlying the energy pileups at both ends of the  $p$ -space scaling range. In the case studied here, they are induced by viscous dissipation and the reduced spectral strength on the scale of the system size, respectively.

PACS numbers: 47.27.-i, 47.10.+g

In nonlinear dynamics scaling exponents in  $r$  space and  $p$  space are often identified with each other. In the case of fully developed turbulence the scaling exponent  $\zeta_{r,2}$  of the velocity structure function  $D^{(2)}(r) = \langle [\mathbf{u}(\mathbf{x} + \mathbf{r}) - \mathbf{u}(\mathbf{x})]^2 \rangle \propto r^{\zeta_{r,2}}$  is believed to coincide with the scaling exponent  $\zeta_{p,2}$  of the energy spectrum of the velocity field (multiplied by  $p$ ),  $E(p) \propto p^{-\zeta_{p,2}-1}$ . In this Letter we demonstrate that this identification only holds in the limit of a very large Reynolds number. For (Taylor-) Reynolds numbers  $\text{Re}_\lambda < 200$  typically achieved in full numerical simulations [1] bottleneck phenomena [2] lead to considerable differences between  $\zeta_{r,2}$  and  $\zeta_{p,2}$ . First, for large  $p$  near the (inverse) scale of dissipation, the bottleneck effect accounts for the puzzling observation that the numerical spectrum is clearly *flatter* both in experiment [3,4] and in numerics [1,5] than  $E(p) \propto p^{-5/3}$  instead of being steeper as expected from the possibility of intermittency corrections. Second, for small  $p$  near the inverse external length scale  $L^{-1}$  (where  $L$  is defined by the driving force), a similar bottleneck effect leads to *steeper* spectra. This is another hint that *finite size effects* as also found and analyzed in [6–9] have to be considered. Our observation has far-reaching consequences for both the numerical and experimental determination of asymptotic scaling exponents from spectra.

We first focus on the crossover between viscous subrange (VSR) and inertial subrange (ISR) and start from Benzi *et al.*'s [10] *measured* longitudinal [11] velocity structure function, assuming that the system size  $L \rightarrow \infty$  [10], i.e., no large scale finite size effects [6,12] are considered. Benzi *et al.* [10] analyzed various numerical and experimental data by means of the extended self-similarity method [10,13] and found that for  $r > \eta$  ( $\eta$  being the Kolmogorov scale) the  $m$ th longitudinal velocity structure function  $D_L^{(m)}(r)$  obeys  $D_L^{(m)}(r) = C_m [rf(r/\eta)]^{\zeta_{r,m}}$ , with a *universal* function  $f(r/\eta)$  for all moments  $m$ , for all  $\text{Re}_\lambda$ , and for all kinds of isotropic flow. We restrict ourselves to the second order structure functions and drop the index 2 in what follows.

The structure functions  $D_L(r)$  and  $D(r)$  are connected by [11]  $D(r) = 3D_L(r) + D_L(r)d \ln D_L(r)/d \ln r$ . Both functions can be fitted by parametrizations of the Batchelor type [11,14]. Originally given by Batchelor as a parametrization, this formula (1) recently got theoretical support by Sirovich, Smith, and Yakhot [8], who, moreover, find agreement between the Batchelor energy spectrum and numerical spectra [1,15] for 30 orders of magnitude. The high quality of the Batchelor fit has also been established by older experiments; for an overview, see [11,16]. Here, the Batchelor fit for  $D(r)$ ,

$$\frac{D(r)}{v_\eta^2} = \frac{r^2/3\eta^2}{[1 + (1/3b)^{3/2}(r/\eta)^2]^{1-\zeta/2}}, \quad (1)$$

is slightly superior to that of  $D_L(r)$ ; see Fig. 1. Here,  $\zeta$  denotes the asymptotic value of  $\zeta_r$  for  $r \gg \eta$ , and  $v_\eta$  and  $b$  are the Kolmogorov velocity and Kolmogorov constant [11], respectively. The experimental value  $f(r = \eta) = 8.577 \times 10^{-3} = f(1)$  determines  $b = 11/45[f(1)]^{2/3} = 5.834$ , slightly smaller than  $b \approx 6.0$ – $8.4$  found in older experiments, which also show excellent agreement with (1) [11,16]. We determine  $D(r)$  from a spline fit to the data and compare the result with the Batchelor parametrization (1) in Fig. 1. There are no visible deviations.

The *local* logarithmic slope [6] of Eq. (1),

$$\zeta(r) = \frac{d \ln D(r)}{d \ln r} = 2 - \frac{(2 - \zeta)r^2}{r_d^2 + r^2}, \quad (2)$$

is *monotonically decreasing* for increasing  $r$ . Here,  $r_d = (3b)^{3/4}\eta$  (for  $\zeta = \frac{2}{3}$ ) determines the  $r$ -space crossover, defined by equating the limits for large and small  $r$  of Eq. (1),  $(r_d/\eta)^2/3 = b(r_d/\eta)^{2/3}$ .

Next, we calculate the spectrum  $E(p)$  which is, when neglecting boundary terms, given by [11,12]

$$E(p) = -\frac{1}{2\pi} \int_0^\infty pr \sin(pr)D(r) dr. \quad (3)$$

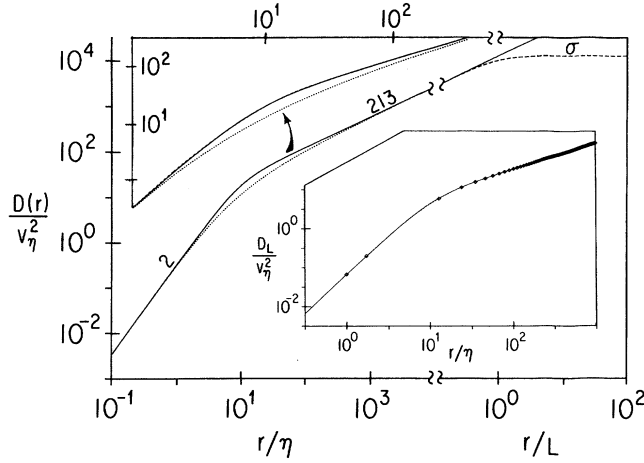


FIG. 1. Velocity structure function  $D(r)$ , calculated from Benzi *et al.*'s data (dashed) [1], and its Batchelor fit (1) (solid) for  $\zeta = \frac{2}{3}$ . Both curves are identical, which can even be seen in the enlargement of the crossover. The dotted line shows a structure function corresponding to the spectrum (6). The upper right part shows the saturation of the structure function (9), dashed. In the inset the longitudinal structure function  $D_L(r)$  is shown. The original data [1] are diamonds, the dashed line is a spline fit of these data, the solid line a fit of Batchelor type. Slight differences are seen.

In view of our results in Fig. 1 we feel justified to consider Eq. (1) as an exact description of the experimental structure function of Ref. [10]. Inserting Eq. (1) into Eq. (3) we obtain

$$E(p) = -\frac{pr_d v_\eta^2}{12\pi\eta^2} \frac{d^3}{dp^3} \int_{-\infty}^{\infty} \frac{\exp(ipr_d x)}{(1+x^2)^{1-\zeta/2}} dx$$

$$= \frac{r_d^3 2^{-1+\zeta/2} v_\eta^2}{3\sqrt{2}\pi \Gamma(1-\zeta/2)\eta^2} [\zeta \tilde{p}^{1/2-\zeta/2} K_{3/2+\zeta/2}(\tilde{p}) + \tilde{p}^{3/2-\zeta/2} K_{1/2+\zeta/2}(\tilde{p})]. \quad (4)$$

Here,  $\tilde{p} = pr_d = p/p_d$  and  $K_\nu(\tilde{p})$  is the modified Bessel function [17]. A similar Fourier transformation of the longitudinal structure function was performed by Sirovich, Smith, and Yakhot [8]. [When the transcriptional error in Eq. (20) of Ref. [8] is corrected, the bottleneck pileup also shows up.] Expanding Eq. (4) for small  $\tilde{p} < 1$  and  $\zeta > 0$  gives

$$\frac{d \ln E(p)}{d \ln p} = -\zeta_p(p) - 1 = \frac{[-\zeta(1+\zeta)\tilde{p}^{1/2-\zeta/2} - \tilde{p}^{5/2-\zeta/2}]K_{3/2+\zeta/2}(\tilde{p}) + (2-\zeta)\tilde{p}^{3/2-\zeta/2}K_{1/2+\zeta/2}(\tilde{p})}{\zeta\tilde{p}^{1/2-\zeta/2}K_{3/2+\zeta/2}(\tilde{p}) + \tilde{p}^{3/2-\zeta/2}K_{1/2+\zeta/2}(\tilde{p})}. \quad (7)$$

For  $\zeta = \frac{2}{3}$  the maximum local slope is  $-1.448$  (instead of  $-5/3$ ) and occurs at  $p_{\min} \approx 0.85p_d \approx (10\eta)^{-1}$ . Figure 3 shows  $\zeta_p(p)$  together with  $\zeta_r(r=1/p)$  from Eq. (2), demonstrating the strikingly different behavior of the local slopes in  $r$  and in  $p$  space.

The energy pileup around  $p_d$  has also been observed in further experiments [3] [fitted by a correction term

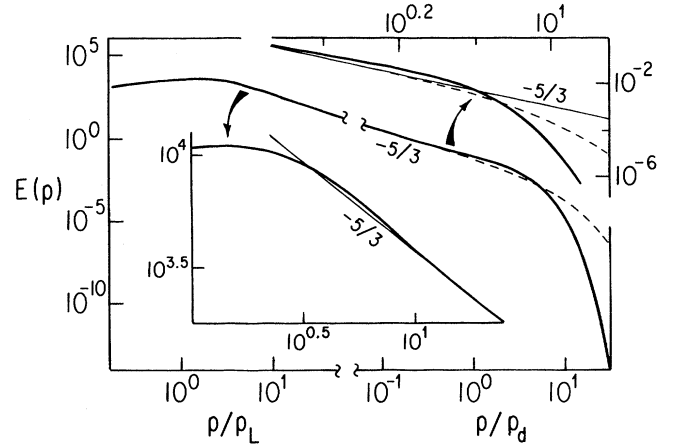


FIG. 2. Experimental energy spectrum Eq. (4) (solid) with  $\zeta = \frac{2}{3}$  and Eq. (6) (dashed) without the energy pileup. In the left part the spectrum according to (10) is shown. In the insets, the spectrum is enlarged around the energy pileups and compared to classical  $-5/3$  scaling.

$$E(\tilde{p}) = \frac{r_d^3 2^{\zeta-1/2} \zeta v_\eta^2}{3\sqrt{2}\pi\eta^2} \frac{\Gamma(3/2 + \zeta/2)}{\Gamma(1 - \zeta/2)}$$

$$\times \tilde{p}^{-\zeta-1} \left[ 1 + \frac{2-\zeta}{2\zeta(1+\zeta)} \tilde{p}^2 + \dots \right], \quad (5)$$

i.e., we have a *positive* correction term to the expected asymptotic scaling  $E(p) \propto p^{-\zeta-1}$ . This correction signals the onset of an *energy pileup* around  $p_d$ ; see Fig. 2. For large  $\tilde{p} \gg 1$  the spectrum decays as  $E(\tilde{p}) \propto \tilde{p}^{1-\zeta/2} \exp(-\tilde{p})$ . Figure 2 also shows a frequently used parametrization [18] for  $E(p)$ ,

$$E(p) = c p^{-\zeta-1} \exp(-p/p'_d), \quad (6)$$

where  $p'_d$  is chosen in such a way that the  $r$ -space crossover  $r'_d$  corresponding to Eq. (6) coincides with  $r_d$ ; for details see Ref. [12]. This comparison emphasizes the energy pileup around  $p_d$  described by the (modified) Sirovich-Smith-Yakhot formula, Eq. (4), which can be considered to an *experimental* spectrum summarizing the various simulations and experiments of Ref. [10] and also those summarized in [16].

As already stated above, the energy pileup leads to a *nonmonotonous* local slope

$\propto p^{2/3}$  instead of our  $p^2$ , cf. Eq. (5)], in full numerical simulations [1,5], and in a reduced wave vector set approximation (REWA) of the Navier-Stokes equations [7]. In Ref. [7] a correction term  $+2(p/p_{\text{peak}})^{1.8}$  was fitted to the data in nice agreement with our present result,  $+3\tilde{p}^2/5 = +2.6(p/p_{\text{peak}})^2$ , where  $p_{\text{peak}}$  is the point of maximum energy dissipation. Falkovich [2]

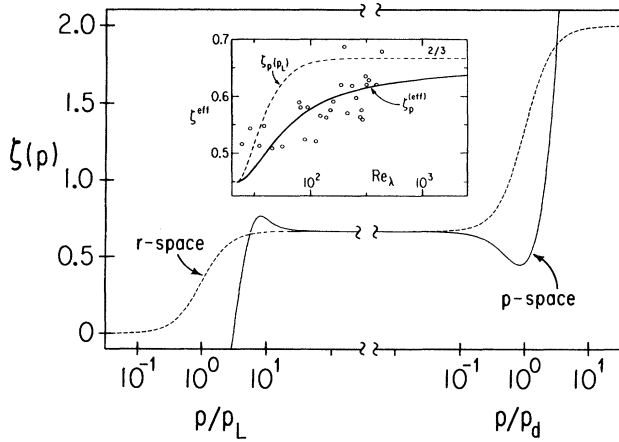


FIG. 3. The local  $p$ -space scaling exponents  $\zeta_p(\bar{p})$  from Eqs. (7) and (10) (solid), and the local  $r$ -space exponent  $\zeta_r(rp_d = 1/\bar{p})$  from Eqs. (2) and (9) (dashed). The inset shows the averaged  $p$ -space scaling exponent  $\zeta_p^{\text{eff}}(\text{Re}_\lambda)$ ; see Eq. (11) (solid). Also shown is the local  $p$ -space scaling exponent  $\zeta_p(p_L(\text{Re}_\lambda))$ , dashed. We chose  $\zeta = \frac{2}{3}$  throughout. The dots are the experimental [5]  $\zeta_p^{\text{eff}}(\text{Re}_\lambda)$ . In [5] only  $\zeta_p^{\text{eff}}(\text{Re})$  is given, so we calculated  $\text{Re}_\lambda = c\text{Re}^{1/2}$  with  $c = 0.17$  chosen to give agreement for small  $\text{Re}_\lambda$ .

introduced the name “bottleneck phenomenon” for the energy pileup and predicts the correction term to be  $\propto (p/p_d)^{4/3}/\ln(p_d/p)$ .

We offer the following *physical* explanation (already given in [7]) of the bottleneck phenomenon: Consider the turbulent energy transfer downscale,  $T(p) \sim pu(\mathbf{p}) \int dp_1 dp_2 u(\mathbf{p}_1)u(\mathbf{p}_2)\delta(\mathbf{p} + \mathbf{p}_1 + \mathbf{p}_2)$ , which does not depend on  $p$  in the inertial range due to Kolmogorov’s structure equation [11]. Assume that the amplitudes  $u(\mathbf{p}_1), u(\mathbf{p}_2)$  with  $p_1, p_2 > p_d > p$  are already damped by viscosity. Then the energy transfer  $T(p)$  would be reduced, and stationarity could not be achieved unless  $u(\mathbf{p})$  increases. Because of the locality of the Navier-Stokes interaction in  $p$  space, the effect is strongest around  $p_d$ , leading to the energy pileup. Of course there is also viscous damping, but for  $p < p_d < \eta^{-1}$  it is smaller than the eddy viscosity  $T(p)$  [2]. Borue and Orszag’s simulations [5] indeed show that the pileup starts in a region where  $T(p)$  is still constant. The above explanation rules out spectra of type (6). For an explanation of the bottleneck effect within the test field model we refer to

Ref. [19]; see also [20]. For an analogous phenomenon in temperature spectra see [21].

*Formally* the bottleneck phenomenon reflects the relatively sharp crossover from  $r^2$  scaling (VSR) to  $r^\zeta$  scaling (ISR) in the structure function (1). To illustrate this we transform the spectrum (6) back to  $r$  space. This spectrum does not show the bottleneck phenomenon, and the corresponding structure function

$$D(r) = \frac{4c\Gamma(-\zeta)}{r(\zeta+1)p_d^{1/\zeta+1}} \{p_d' r(\zeta+1) - (1+p_d'^2 r^2)^{(\zeta+1)/2} \sin[(\zeta+1)\arctan(p_d' r)]\} \quad (8)$$

differs from the Batchelor parametrization (1) by its considerably *smoother* transition (see the dotted curve in Fig. 1, showing a ratio of  $\approx 1.8$  around  $r_d$ ).

Our explanation suggests that the bottleneck effect potentially accompanies any sudden change in spectra strength, provided the wave vector amplitudes interact nonlinearly and a conserved flux exits. We are consequently led to expect a similar effect at the infrared end of the scaling regime where the small- $p$  modes are reduced in their spectra strength by the finite system size.

Let us therefore consider the crossover between ISR and the large  $r$  saturation domain, where  $D(r) = 2\langle u^2 \rangle = 6u_{1,\text{rms}}^2$  becomes constant. Recall that  $L \equiv 1/p_L$  is the forcing scale. From experimental data [10,11,16] we conclude that the second crossover at  $r = L$  is again well described by a Batchelor type transition,

$$D(r) = 2\langle u^2 \rangle r^2 (r_d^2 + r^2)^{-1+\zeta/2} (L^2 + r^2)^{-\zeta/2}; \quad (9)$$

see Fig. 1. [This crossover is probably nonuniversal. The important point here is simply the reduced spectral strength for small  $p$ , induced by the finite size, i.e.,  $E(p) \rightarrow 0$  as  $p \rightarrow 0$ .] The general mechanism outlined above should apply equally well in this regime: The velocity amplitudes of the modes  $p_1, p_2 < p_L < p$  (or either of them) are reduced because of the finite size of the system. The mode  $u(\mathbf{p})$  again has to increase in order to guarantee a  $p$ -independent energy flux, now resulting in a *steeper* spectrum.

Indeed, we find such a behavior for the spectrum corresponding to (9). For  $r_d \ll r$  we derive the analytical result (for  $\zeta = \frac{2}{3}$ )

$$E(p) = \frac{\langle u^2 \rangle L}{\pi} \left\{ -\frac{\Gamma(5/6)}{\Gamma(1/3)} \sqrt{\pi} \left[ \frac{5}{9} \bar{p}^2 {}_1F_2\left(\frac{11}{6}, \frac{5}{2}, \frac{5}{2}, \frac{\bar{p}^2}{4}\right) + \frac{11}{405} \bar{p}^4 {}_1F_2\left(\frac{17}{6}, \frac{7}{2}, \frac{7}{2}, \frac{\bar{p}^2}{4}\right) \right] + \frac{\pi}{2} \left[ \frac{1}{3} \bar{p} {}_1F_2\left(\frac{4}{3}, 2, \frac{3}{2}, \frac{\bar{p}^2}{4}\right) + \frac{2}{27} \bar{p}^3 {}_1F_2\left(\frac{7}{3}, 3, \frac{5}{2}, \frac{\bar{p}^2}{4}\right) \right] \right\}, \quad (10)$$

where  $\bar{p} = p/p_L$  and  ${}_1F_2(a, b, c, z)$  denotes a generalized hypergeometric function [17]. The spectrum and the corresponding  $\zeta_p(p)$  are shown in the left parts of Figs. 2 and 3, respectively. We find  $p_{\text{max}} \approx 8p_L$  and  $\zeta(p_{\text{max}}) \approx 0.77$ . Thus the deviations from classical scaling are again much larger than the discussed intermittency corrections. Note that

our result agrees with theoretical [6,9] and experimental hints (summarized in [9]) that the spectra are steeper for small  $p$ .

We finally calculate the *effective* scaling exponent  $\zeta_p^{(\text{eff})}(\text{Re}_\lambda)$  that will be measured in  $p$ -space simulations. Here we only consider the bottleneck phenomenon for large  $p$ , as in most numerical schemes the smallest wave vectors are forced and no  $p < p_L$  are included. Let us express  $r_d$  in terms of  $L$  and the Taylor-Reynolds number  $\text{Re}_\lambda = \lambda u_{1,\text{rms}}/\nu$ , where  $\lambda = u_{1,\text{rms}}/(\partial_1 u_1)_{\text{rms}}$  is the Taylor length. We have  $\epsilon = c_\epsilon u_{1,\text{rms}}^3/L$  with  $c_\epsilon = (6/b)^{3/2} \approx 1$ , which is also known from grid turbulence experiments [22]. On the other hand,  $\epsilon = 15\nu(\partial_1 u_1)_{\text{rms}}^2$  [11]. Using these relations we finally get  $\eta = 15^{3/4} c_\epsilon^{-1} L \text{Re}_\lambda^{-3/2}$  or (for  $\zeta = \frac{2}{3}$ )  $r_d = (3b)^{3/4} \eta \approx 63L \text{Re}_\lambda^{-3/2}$ . This connection between  $r_d/L$  and  $\text{Re}_\lambda$  allows us to calculate  $\zeta_p^{(\text{eff})}(\text{Re}_\lambda)$  as the average

$$\zeta_p^{(\text{eff})}(\text{Re}_\lambda) = \frac{1}{\ln(p_{\text{min}}/p_L)} \int_{p_L}^{p_{\text{min}}} \zeta_p(p) d \ln p, \quad (11)$$

where  $p_{\text{min}}$  is, as above, the wave vector of minimal  $\zeta_p(p)$ . The function  $\zeta_p^{(\text{eff})}(\text{Re}_\lambda)$  is shown in the inset of Fig. 3. The deviations from the asymptotic value  $\zeta_p^{(\text{eff})}(\text{Re}_\lambda \rightarrow \infty) = \zeta$  are large. Assuming  $\zeta = \frac{2}{3}$ , even for the largest  $\text{Re}_\lambda = 200$  achieved in numerical simulations [1] we have  $\zeta_p^{(\text{eff})} \approx 0.58$ , which very well agrees with what is observed in numerical simulations [1]. Impressive *experimental* confirmation of our prediction follows from recent measurements by Zocchi *et al.* [4]. We include their data for  $\zeta_p^{(\text{eff})}(\text{Re}_\lambda)$  in our figure.

Let us finally remark that our physical explanation of the bottleneck energy pileups is very general; it only assumes some inertial range with a constant energy flux in  $p$  space. For example, these conditions hold for surface or capillary waves [23], where bottleneck phenomena are also expected [2], or for Kuramoto-Sivashinsky dynamics [24]. How bottleneck phenomena manifest themselves in higher order moments and in power spectra remains a question for further research.

We are grateful to R. Benzi, who kindly supplied us with his experimental data. We thank him and M. Brenner, S. Esipov, A. Esser, G. Falkovich, A. Golubentsev, S. Grossmann, J. Herring, M. Jensen, L. Kadanoff, R. Kerr, S. Kida, A. Praskovsky, and L. Sirovich for discussions and hints. D.L. acknowledges support by a NATO grant through the Deutsche Akademische Austauschdienst (DAAD) and by DOE. A.M.-G. was supported by NSERC.

\*On leave of absence from Fachbereich Physik, Universität Marburg, Renthof 6, D-35032 Marburg, Germany.

†Present address: C.E.A., Service de Physique de l'État Condensé, Centre d'Études de Saclay, 91191 Gif sur Yvette Cedex, France.

- [1] Z. S. She, S. Chen, G. Doolen, R. H. Kraichnan, and S. A. Orszag, Phys. Rev. Lett. **70**, 3251 (1993); A. Vincent and M. Meneguzzi, J. Fluid Mech. **225**, 1 (1991); R. Kerr, J. Fluid Mech. **211**, 309 (1990).
- [2] G. Falkovich, Phys. Fluids **6**, 1411 (1994).
- [3] Z. S. She and E. Jackson, Phys. Fluids A **5**, 1526 (1993); S. G. Saddoughi and S. V. Veeravalli, J. Fluid Mech. **268**, 333 (1994); also C. Wark (private communication).
- [4] G. Zocchi, P. Tabeling, J. Mauerer, and H. Willaime, Phys. Rev. E **50**, 3693 (1994).
- [5] D. Porter, P. Woodward, and A. Pouquet, "Inertial Range Structures in Compressible Turbulent Flows" (to be published), V. Borue and S. A. Orszag, "Forced 3D Homogenous Turbulence with Hyperviscosity" (to be published).
- [6] S. Grossmann and D. Lohse, Phys. Fluids **6**, 611 (1994); S. Grossmann, D. Lohse, V. L'vov, and I. Procaccia, Phys. Rev. Lett. **73**, 432 (1994); V. S. L'vov and I. Procaccia, Phys. Rev. E **49**, 4044 (1994).
- [7] S. Grossman and D. Lohse, Phys. Rev. E **50**, 2784 (1994).
- [8] L. Sirovich, L. Smith, and V. Yakhot, Phys. Rev. Lett. **72**, 344 (1994).
- [9] V. Yakhot, Phys. Rev. E **49**, 2887 (1994).
- [10] R. Benzi, S. Ciliberto, C. Baudet, and G. R. Chavarria, "On the Scaling of 3D, Homogeneous, Isotropic, Turbulence," Physica D (Amsterdam) (to be published).
- [11] A. S. Monin and A. M. Yaglom, *Statistical Fluid Mechanics* (The MIT Press, Cambridge, Massachusetts, 1975).
- [12] D. Lohse and A. Müller-Groeling, "Anisotropy and Scaling Corrections in Turbulence (to be published).
- [13] R. Benzi, S. Ciliberto, R. Tripicciono, C. Baudet, F. Massaioli, and S. Succi, Phys. Rev. A **48**, R29 (1993).
- [14] G. K. Batchelor, Proc. Camb. Philos. Soc. **47**, 359 (1951).
- [15] S. Chen, G. D. Doolen, J. R. Herring, R. H. Kraichnan, S. A. Orszag, and Z. S. She, Phys. Rev. Lett. **70**, 3051 (1993).
- [16] H. Effinger and S. Grossmann, Z. Phys. B **66**, 289 (1987).
- [17] M. Abramowitz and I. A. Stegun, *Handbook of Mathematical Functions* (Dover, New York, 1970); A. P. Prudnikov, Yu. A. Brychkov, and O. I. Marichev, *Integrals and Series* (Gordon and Breach, New York, 1990), Vol. 3.
- [18] C. Foias, O. Manley, and L. Sirovich, Phys. Fluids A **2**, 464 (1990).
- [19] J. R. Herring, D. Schertzer, M. Lesieur, G. R. Newman, J. P. Chollet, and M. Larcheveque, J. Fluid Mech. **124**, 411 (1982).
- [20] J. Qian, Phys. Fluids **27**, 2229 (1984).
- [21] V. I. Tatarskii, M. M. Dubovikov, A. A. Praskovsky, and M. Y. Karyakin, J. Fluid Mech. **238**, 683 (1992).
- [22] K. R. Sreenivasan, Phys. Fluids **27**, 1048 (1984). We neglected the  $\text{Re}_\lambda$  dependence of  $c_\epsilon$ , cf. D. Lohse, Phys. Rev. Lett. **73**, 3223 (1994).
- [23] V. E. Zakharov, V. S. L'vov, and G. Falkovich, *Kolmogorov Spectra of Turbulence* (Springer, Heidelberg, 1992).
- [24] Y. Kuramoto, Suppl. Prog. Theor. Phys. **64**, 346 (1978); G. Sivashinsky, Acta Astronautica **4**, 1177 (1977).